

Document downloaded from:

<http://hdl.handle.net/10251/150641>

This paper must be cited as:

Catalá-Icardo, M.; Torres-Cartas, S.; Simó-Alfonso, EF.; Herrero-Martínez, JM. (2020). Influence of photo-initiators in the preparation of methacrylate monoliths into poly(ethylene-co-tetrafluoroethylene) tubing for microbore HPLC. *Analytica Chimica Acta*. 1093:160-167. <https://doi.org/10.1016/j.aca.2019.09.055>



The final publication is available at

<https://doi.org/10.1016/j.aca.2019.09.055>

Copyright Elsevier

Additional Information

**Influence of photo-initiators in the preparation of methacrylate monoliths into
poly(ethylene-co-tetrafluoroethylene) tubing for microbore HPLC**

M. Catalá-Icardo¹, S. Torres-Cartas¹, E.F. Simó-Alfonso², J.M. Herrero-Martínez²

¹ *Instituto de Investigación para la Gestión Integrada de Zonas Costeras, Campus de Gandía, Universitat Politècnica de València, C/ Paranimf 1, 46730 Grao de Gandía, Valencia, Spain*

² *Department of Analytical Chemistry, Universitat de València, Dr. Moliner 50, 46100 Burjassot, Valencia, Spain*

*Corresponding authors: Dr. José Manuel Herrero-Martínez

Tel.: +34963544062

Fax: +34963544436

e-mail: jmherrer@uv.es

Dr. Mónica Catalá-Icardo

Tel.: +34 96 284 93 33

Fax: +34 96 284 93 09

e-mail: mocaic@qim.upv.es

Abstract

In this study, poly(butyl methacrylate-*co*-ethylene glycol dimethacrylate) polymeric monoliths were *in situ* developed within 0.75 mm i.d. poly(ethylene-*co*-tetrafluoroethylene) (ETFE) tubing by UV polymerization via three different free-radical initiators (α,α' -azobisisobutyronitrile (AIBN), 2,2-dimethoxy-2-phenylacetophenone (DMPA) and 2-methyl-4'-(methylthio)-2-morpholinopropiophenone (MTMPP). The influence of the nature of each photo-initiator and irradiation time on the morphological features of the polymer was investigated by scanning electron microscopy, and the chromatographic properties of the resulting microbore columns were evaluated using alkyl benzenes as test substances. The beds photo-initiated with MTMPP gave the best performance (minimum plate heights of 38 μm for alkyl benzenes) and exhibited a satisfactory reproducibility in the chromatographic parameters (RSD < 11%). These monolithic columns were also successfully applied to the separation of phenylurea herbicides, proteins and a tryptic digest of β -casein.

Keywords: Photografting; photo-initiator; poly(ethylene-*co*-tetrafluoroethylene); polymer monolith; reversed-phase liquid chromatography

1. Introduction

In recent decades, the number of analytical applications of organic polymer-based monoliths has grown progressively, covering innovations chromatography and sample preparation fields [1-3]. The key to success lies in their simple preparation, high permeability, tunable properties, and easily available surface chemistries. The polymerization reaction to synthesize these materials can be initiated by different strategies, being thermal [4, 5] and photoinduced [6, 7] modes the most usual ones. Within photopolymerization modes, UV irradiation has been the most common way, although another type of electromagnetic radiation has also been used [8]. Unlike thermal polymerization, UV initiation is significantly fast (performed in few minutes) with low energy requirements and cost. An additional advantage of this initiating way is the possibility of controlling the monolithic formation within a specific space of support (capillary or microchip) using a mask to restrict the irradiation onto the selected area [8-12].

Typically, the morphological features of the polymeric monoliths, and therefore their chromatographic performance, are influenced by both the composition of the polymeric mixture, including porogen solvent selection, monomer/porogen solvent ratio, nature and concentration of initiator, and the strategy used to initiate the polymerization, such as wavelength and intensity of the light in the UV polymerization [9, 13]. However, few studies have investigated the behavior of different photo-initiators on the preparation of polymer-based monoliths [12-14], being all of them performed on miniaturized supports (capillary or microchip).

When a free radical UV photo-initiator is used in the polymerization mixture, the presence of the UV light (usually at 254 or 365 nm) leads to the decomposition of the initiator into free radicals, following either a scission or hydrogen abstraction process

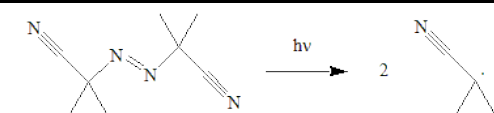
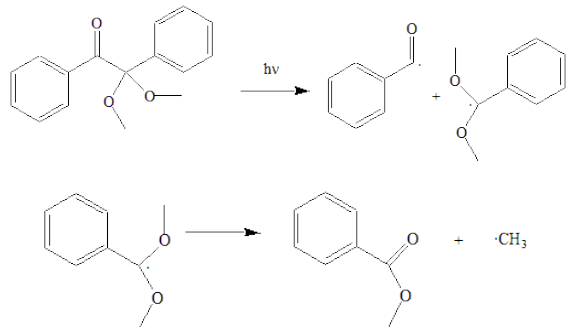
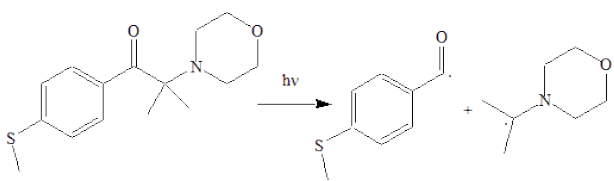
mechanism [15]. In both cases, the amount of radicals obtained, is affected both by the medium as well as the nature of the photoinitiator. Also, the efficiency of a photoinitiator depends on its absorption spectrum (absorption bands and the corresponding extinction coefficients, ϵ) [14, 16], Thus, a large amount of initiated polymer nuclei could be obtained by a conjunction of high ϵ at the irradiation wavelength, high dissociation quantum yields and reactivity of the key radicals towards the monomer.

Among UV photo-initiators employed to prepare polymeric monoliths, α,α' -azobisisobutyronitrile (AIBN) has been used to conduct this process at 365 nm (close to its maximum absorption [17]), and at 254 nm [13, 18]. Another photoinitiator widely used is 2,2-dimethoxy-2-phenylacetophenone (DMPA or Irgacure 651) [19-22]. In this case, both 254 nm (maximum absorption band) and 365 nm have been selected as irradiation wavelengths. However, other photo-initiators such as 2-methyl-4'-(methylthio)-2-morpholinopropiophenone (MTMPP or Irgacure 907) have been scarcely employed [14]. For this initiator, the main irradiation wavelength was 365 nm [23]. Table 1 depicts the cleavages routes for the three initiators mentioned [13, 24] as well as their molar extinction coefficients (ϵ) and quantum yields (Φ).

On the other hand, monolithic columns obtained by UV initiation have been usually prepared in fused-silica capillaries with UV-transparent external coating, which are more expensive than conventional polyimide coated capillaries. In this sense, the use of UV transparent housing materials economically feasible and available in different sizes and formats will be desirable. Recently, we have reported [5] the use of fluoropolymers as new supporting materials for polymeric monolithic stationary phases. In particular, poly(ethylene-*co*-tetrafluoroethylene) (ETFE) has showed outstanding chemical resistance, suitable mechanical features, transparency to UV radiation and the presence

of abstractable hydrogens in its structure provides a stable covalent attachment of the monolith to the fluoropolymer wall by photo-grafting process.

Table 1. Photolytic cleavages schemes of the three photo-initiators studied: (A) AIBN; (B) DMPA; (C) MTMPP. Dissociation quantum yields (Φ) and extinction coefficients at maximum wavelength of each initiator were also included [14, 24, 31].

Initiator	Absorption λ (nm)	Extinction coefficient ϵ ($L \cdot mol^{-1} \cdot cm^{-1}$)	Quantum yield (Φ)	Photolytic cleavages scheme
AIBN	345	11.9	0.4	
DMPA	343	242	1.71	
MTMPP	303	18 600	0.88	

In this work, the synthesis of butyl methacrylate (BMA)-based monoliths in ETFE tubing (0.75 mm i.d.) by photo-polymerization with three different photo-initiators (AIBN, DMPA and MTMPP) is described. The influence of each type of initiator and the irradiation time on the resulting monolithic beds was fairly investigated. The morphology of the microbore monolithic supports was studied by scanning electron microscope

(SEM) images, and the chromatographic behaviour was evaluated by means of retention factors and separation performance of a mixture of alkyl benzenes. Besides, the reproducibilities of monolithic columns were evaluated. In addition, the photopolymerized monoliths in ETFE tubing were successfully applied to the separation of phenylurea herbicides, proteins, and a tryptic digest of casein in a conventional HPLC system. To the best of our knowledge, the work presented herein described for the first time the use of ETFE tubing as supporting material to obtain microbore monolithic columns produced by UV initiation including a careful choice of photoinitiator for free radical photopolymerization.

2. Materials and methods

2.1. Chemicals and reagents

Butyl methacrylate (BMA), ethyleneglycol dimethacrylate (EDMA), 1,4-butanediol, 1-propanol, 2,2-dimethoxy-2-phenylacetophenone (DMPA, Irgacure 651) and 2-methyl-4'-(methylthio)-2-morpholinopropiophenone (MTMPP, Irgacure-907) were from Sigma-Aldrich (Steinheim, Germany). α,α' -Azobisisobutyronitrile (AIBN) was from Fluka (Buchs, Switzerland). Benzophenone (BP) was obtained from Alfa Aesar (Karlsruhe, Germany). , Acetonitrile (ACN) and methanol (MeOH), of HPLC grade were purchased from Merck (Darmstadt, Germany). Alkyl benzenes, uracil, diuron, monuron and linuron from Riedel de Haën (Seelze, Germany), Chlorotoluron from Chem Service (West Chester, PA, USA) and cytochrome C (bovine pancreas) and ribonuclease A (bovine heart) were from Alfa Aesar. Trypsin from bovine pancreas, myoglobin (horse skeletal muscle) and β -casein (bovine milk) were purchased from Sigma.

A water purification system Purity TU6 from VWR (Bedford, MA, USA) was employed to obtain ultra-pure water (a 0.2 μm filter was included) ETFE tubing of 1/16'' (1.6 mm o.d. \times 0.75 mm i.d.) from Vici Jour (Schenkon, Switzerland) was used.

Stock solutions (1.0 mg mL^{-1}) of alkyl benzenes in ACN were prepared and kept at 4°C until their use. Stock solutions of phenyl urea herbicides and proteins were prepared at 1.0 mg mL^{-1} in ACN or water, respectively, and kept at -20°C until their use. Working standard solutions were prepared daily before the analysis with ultra pure-water for proteins and the corresponding mobile phase for the rest of compounds.

2.2. Instrumentation

Photografting and photo-polymerization processes were conducted using an UV crosslinker (model CL1000) from UVP (Upland, CA, USA) provided with UV lamps (5 \times 8W, 254 nm) or (5 \times 8W, 365 nm), respectively. Reagents were introduced into the tubing by means of a syringe pump (Model 100, KD Scientific, New Hope, PA, USA). A scanning electron microscope (S-4800, Hitachi, Ibaraki, Japan) with a field emission gun, and an EMIP 3.0 image data acquisition system was employed to obtain SEM photographs. To avoid charging problems, the polymeric sorbents were sputter-coated with Au/Pd for 2 min. Nitrogen adsorption–desorption isotherms were measured at 77 K using a TriStar II (Micromeritics) gas adsorption analyzer. In order to establish the specific surface area, data were analyzed by using the Brunauer-Emmett-Teller model (BET).

An HPLC from Jasco Analytica (Madrid, Spain), containing a PU-2089 quaternary gradient pump, an AS-2055 autosampler and a MD-2018 photodiode array detector, was employed. The interface LC-NETII/AFC (Jasco Analytical) allowed the control of the system, and the ChromNAV software (version 1.17.01), the acquisition and data

treatment.

2.3. Preparation of polymer monoliths

To ensure covalent attachment of monolithic beds to the inner ETFE wall, a two-step photo-grafting procedure previously described in our research group [5] was carried out. Briefly, the ETFE tube was filled with a solution of 5 wt% of BP in MeOH (previously deoxygenated), and then it was irradiated for 20 min under 254 nm at 0.9 J cm^{-2} . Next, a deaerated solution composed of 15 wt% of EDMA in MeOH was used to flush the modified Teflon tubing, and treated as above.

The selected polymerization mixture was composed of: 24 wt% BMA as monomer, 16 wt% EDMA as cross-linker, 60 wt% of a ternary pore-forming solvent (18 wt% 1,4-butanediol, 37 wt% 1-propanol and 5 wt% water), and 1 wt% (respect the total monomers amount) of initiator. Various monolithic columns were synthesized using three different initiators (AIBN, DMPA and MTMPP) at several irradiation times. The mixtures were sonicated for 5 min and next purged with nitrogen for 10 min. The EDMA-modified ETFE tubing was then filled with the polymerization solution, its two ends were sealed with caps, and the tube was irradiated at 0.9 J cm^{-2} , being 2.5 cm the distance selected between the tube and the lamps. The photo-polymerization was performed at 365 nm in all cases, and also at 254 nm for AIBN. After polymerization, the column was cut to 10 cm long, fitted with end fittings to allow connection to the HPLC pump and flushed firstly with MeOH to remove the possible unreacted monomers and the pore-forming solvents, and next with the mobile phase.

2.4. Preparation of tryptic digest of β -casein

The tryptic digest of β -casein was prepared as previously described [25]. Briefly, β -casein

was prepared at a concentration of 2.5 mg/mL in a solution of ammonium bicarbonate (10 mmol/L at pH 8.2. Then, trypsin was added at a substrate-to-enzyme ratio of 50:1 w/w and the solution was incubated at 37°C for 20 h. The addition of 10% acetic acid was done to stop the proteolysis.

3. Results and discussion

3.1. Preparation and characterization of butyl methacrylate columns photo-initiated with AIBN in ETFE tubing

Using AIBN, a series of BMA-monolithic columns were prepared under two irradiation wavelengths (254 and 365 nm) by modifying the irradiation time (between 10 and 50 min) and using 0.9 J/cm² as irradiation energy (maximal allowed by the UV crosslinker). The preparation of BMA-based monoliths was adapted from a previously work [5]. As shown in Table 2, at 254 nm, an increase in the irradiation time from 20 to 40 min led to a decrease in permeability and an increase in retention (*k*-values). SEM photographs of these monoliths were done to interpret this behaviour, (Fig. S1). A higher number of clusters with lower size was evidenced from 20 to 40 min, which results in an increase in surface area of resulting polymer from 5.2 m²·g⁻¹ (at 20 min) to 16.3 m²·g⁻¹ (at 40 min), and thereby, larger retention. It would be feasible to assume that increasing the irradiation time (from 20 to 40 min) increases the polymerization rate (or reaction kinetics), which would generate a higher number of free-radicals and growing agglomerates, which would therefore produce smaller globules. On the other hand, irradiation times longer than 40 minutes did not lead to significant changes in retention factors. A possible explanation of this fact could be due to “self-screening” of the UV radiation by the nuclei or globules already formed during UV-curing [13].

Table 2. Chromatographic properties of BMA-based monolithic columns prepared with several photo-initiators^a.

Init.	Irrad. time (min)	Permeab. (μm^2) ^b	Poros ^c	Pres. (MPa)	Surface area ($\text{m}^2\cdot\text{g}^{-1}$)	k_{tol}	k_{prop}	k_{pent}	Global resolution ^d
AIBN	20	0.365	4.40	0.30	5.2	1.11	3.84	15.27	- ^e
(254 nm)	30	0.222	4.34	0.50	7.1	1.36	4.62	18.39	- ^e
	40	0.130	4.25	0.85	16.3	1.91	6.60	24.54	2.22
	50	0.128	4.18	0.90	16.5	1.92	6.56	24.32	2.14
AIBN	10	0.081	4.28	1.40	18.3	2.10	7.41	27.24	3.08
(365 nm)	20	0.050	4.21	2.30	21.1	2.55	9.26	34.77	2.73
	30	0.047	4.15	2.50	27.4	3.25	11.98	44.58	2.56
DMPA	2	0.066	4.18	1.75	17.3	1.96	6.67	24.74	1.97
(365 nm)	5	0.035	4.17	4.00	19.8	2.01	7.67	29.34	3.59
	10	0.027	4.25	4.20	23.5	2.27	7.74	28.28	3.52
	20	0.029	4.12	4.10	24.3	2.60	9.42	32.84	2.52
	30	0.026	4.18	4.40	21.1	2.32	7.88	28.60	2.57
MTMPP	5	0.113	4.37	1.05	8.4	1.26	4.79	18.22	2.81
(365 nm)	10	0.070	4.25	1.65	19.8	1.91	7.57	26.91	2.74
	20	0.036	4.15	3.20	24.3	2.42	8.60	31.55	2.52
	30	0.031	4.18	3.70	21.3	2.07	7.41	27.98	1.45

^a Initiator content used: 1 wt% with respect to the monomers.

^b Evaluated as $K=L \eta u / \Delta P$, where L is the length of the column, η is the viscosity of the mobile phase (32:68, v/v ACN:H₂O), u is the linear flow velocity, and ΔP is the backpressure of the column.

^c Evaluated as $\varepsilon_T = V_M / V_C$, where V_M is the elution volume of the non-retained uracil and V_C is the overall volume of the empty cylindrical column.

^d Calculated as geometrical mean of resolution between the consecutive alkyl benzene pairs.

^e All peaks were overlapped

The global resolution (evaluated as the geometrical average of the resolution between adjacent alkylbenzene peaks) and efficiency of the different columns were also examined (see Table 2 and Fig. 1A, respectively). As it can be seen, an irradiation time of 40 min gave the best performance, and this time was selected for subsequent studies.

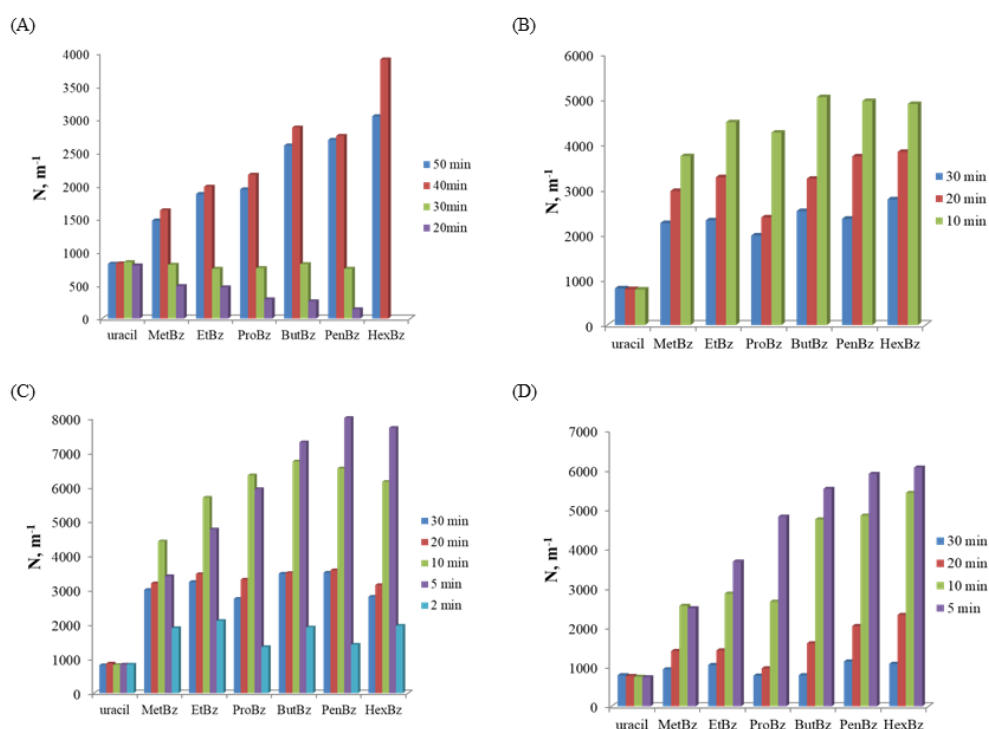


Fig. 1. Effect of irradiation time over the efficiency (N) of the BMA-based monolithic columns prepared with the three photo-initiators studied: (A) AIBN at 254 nm; (B) AIBN at 365 nm; (C) DMPA at 365 nm; and, (D) MTMPP at 365 nm. Experimental conditions: ETFE tubing, 100 mm \times 0.75 mm i.d.; mobile phase, 32:68 (v/v) ACN:H₂O; flow rate, 0.14 mL min⁻¹; injection volume, 1 μ L; UV at 214 nm.

Then, the behaviour of this initiator at 365 nm (close of its maximum absorption wavelength, see Table 1) was also considered. As shown in Table 2, a similar trend in terms of permeability and k -values with irradiation time to that observed at 254 nm was found. These results were also consistent with SEM images of these beds (Fig. S1, parts C-D). However, at 365 nm, short irradiation times (10 min) were enough to provide monoliths with satisfactory separation performance (see Table 2 and Fig. 1B). Exposure times longer than 20 minutes gave rise to a significant reduction in permeability, which resulted in very long retention times. These results were consistent with the total porosity and surface values obtained (see Table 2).

The differences found between photo-initiated monoliths with AIBN at two different wavelengths can be explained in terms of optimal energy absorption of the initiator [26]. Thus, when its spectrum is matched with UV-lamp emission maximum, an efficient UV curing of polymer monolith is achieved. In this sense, AIBN presents a maximum absorption close to 365 nm, and therefore, its decomposition rate is more effective, giving as result the production of a large amount of free-radicals and growing nuclei, which would lead to smaller globules. Indeed, at a given exposure time, the beds initiated at this wavelength showed globule sizes smaller than those obtained at 254 nm (see Fig. S1A and S1D). As shown in Table 2, the monoliths photo-initiated at 365 nm for 10 min provided better efficiency and resolution values than those synthesized for longer exposure times. Accordingly, 10 min was established for further studies.

Fig. 2A and 2B show the isocratic separation of alkylbenzenes obtained with monolithic columns prepared at the optimum irradiation times: 40 and 10 min at 254 and 365 nm, respectively. The photo-initiated column prepared at 365 nm gave much better efficiencies (ranged 75-146 μm , values obtained from the van Deemter plot) than the column prepared at 254 nm (plates heights within 186-230 μm).

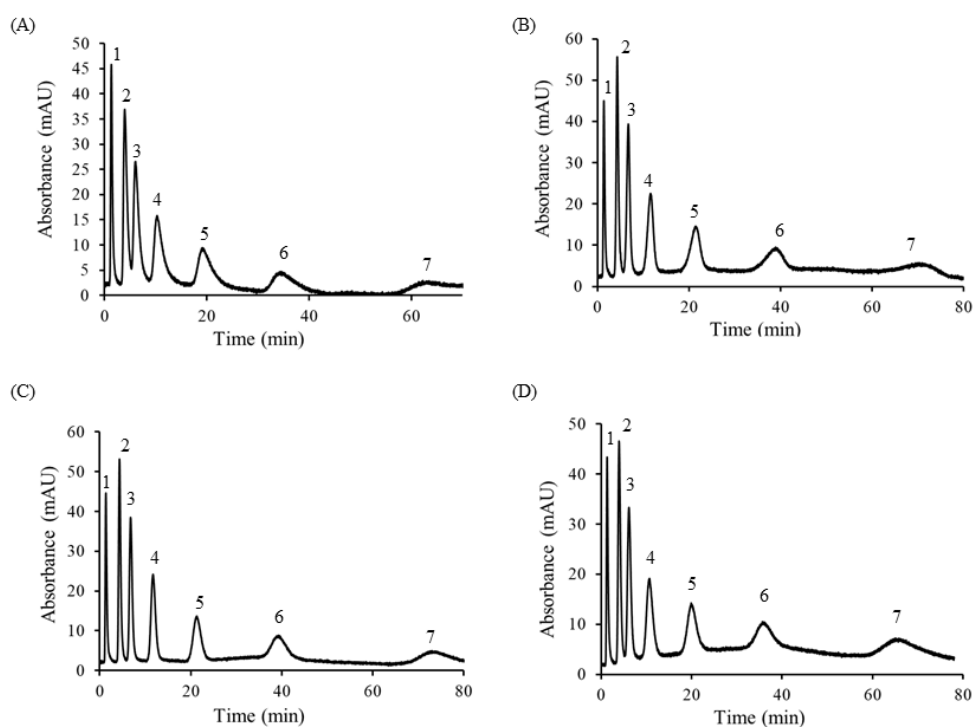


Fig. 2. Separation of alkyl benzenes obtained using BMA-based monolithic columns prepared with the three photo-initiators studied (at their optimal exposure time): (A) AIBN at 254 nm (40 min of irradiation time); (B) AIBN at 365 nm (10 min); (C) DMPA at 365 nm (10 min); and, (D) MTMPP at 365 nm (5 min). Working LC conditions as in Fig. 1. Peak identification: uracil (1), toluene (2), ethylbenzene (3), propylbenzene (4), butylbenzene (5), pentylbenzene (6) and hexylbenzene (7). Other details about the composition of the columns are given in Experimental section.

3.2. Preparation and characterization of butyl methacrylate columns photo-initiated with DMPA or MTMPP in ETFE tubing

BMA-based monolithic columns using DMPA as photo-initiator and the same polymerization solution mentioned above were prepared by varying the exposure time. On the basis of previous studies done with AIBN, the output wavelength of UV lamp was selected close to the absorption spectrum maximum wavelength of initiator. Thus, for a DMPA, an output wavelength of 365 nm was chosen [14]. As shown in Table 2, an increase in irradiation time from 2 to 20 minutes resulted in a progressive increase in

retention factors, whereas longer irradiation times led to a decrease of retention. On the other hand, the permeability decreased when exposure time raised from 2 to 5 min, remaining practically constant for longer times. SEM photographs (see Fig. S2A as representative example) of all these monoliths were taken; however, they did not exhibit significant changes in morphology. These evidences are consistent with previous findings described in the literature [13] and can be justified by considering the large efficiency of DMPA as initiator, which translates into a fast polymerization rate of nuclei (as we explain below), being enough 5 or 10 min to achieve the formation of well-developed monoliths. The application of longer irradiation times did not show apparently a significant effect on the polymer network structure. Indeed, similar total porosity values and surface areas were obtained for synthesized DMPA-based monoliths (see Table 2).

As shown in Table 2, the columns obtained both at 5 and 10 min of irradiation time offered large efficiency and global resolution values, although the monolithic column prepared with 10 min gave better reproducibility, and it was selected for further studies. Fig. 2C shows the chromatogram of alkyl benzenes obtained with the monolithic columns prepared with DMPA under an exposure time of 10 min. Satisfactory efficiencies (minimum plate heights within the 40-76 μm range obtained from the van Deemter plot) were obtained.

The possibility of using other acetophenone-type initiator, MTMPP, as free-radical source instead of DMPA was also considered. Thus, a set of monolithic columns were prepared under different irradiation times (between 5 and 30 min). Also, in this case, irradiation experiments were done with a light source emitting at 365 nm (see Table 1 for absorption band of MTMPP). The studies showed that an increase in the irradiation time from 5 to 20 minutes led to a decrease in permeability together with an increase in k -values. This fact can be explained due to the presence of a lower globule size along this

time range, as it can be seen in SEM photographs (see Fig. S2B-C), and also in the surface area values (see Table 2). These findings were consistent with results described by Araya-Farias *et al.* [14]. However, irradiation times longer than 20 minutes led to a diminution in the k -values, which can be owing to the large globule size (see Fig. S2D). Several possible explanations could be given for this behavior. On the one hand, as we mentioned in a previous section, a screening effect could take place. On the other hand, several authors [27] have reported that longer irradiation times can produce de polymerization reactions leading to the reappearance of monomer molecules, and consequently the formation of a poorly developed polymer.

Also, the performance of the columns prepared with MTMPP was evaluated (see Table 2 and Fig. 1D), obtaining the best results for those irradiated for 5 min, which was selected for subsequent studies. Fig. 2D shows the chromatogram of alkyl benzenes belonging to the monolithic columns prepared using MTMPP under 5 min of irradiation time. Minimum plate height values between 38 and 124 μm were obtained (from the van Deemter plot) for these UV-polymerized monoliths.

3.3. Comparison performance of photo-initiators

The results shown above for monoliths with different photo-initiators can be explained bearing in mind the following considerations. In addition to the nucleation mechanism, it should be considered that the efficiency of the initiation process and generation of radicals relies on the photo-initiator type used. Indeed, each initiator has its particular radical generation rate, which depends on several factors such as the quantum yield of dissociation (Φ), the wavelength-dependent ϵ , the spectral photon flux, the photo-initiator concentration, among others. [16]. As shown in Table 1, MTMPP presents the highest radical generation rate of all tested photo-initiators at 365 nm due to a fruitful

combination of a high Φ value (0.85) and extinction coefficient ($18600 \text{ L mol}^{-1} \text{ cm}^{-1}$) [14]. According to Araya-Farias *et al.* [14], it can be related to the presence of nitrogen on its chemical structure (see Table 1), which provides a higher electron density on the α -carbon atom, thus allowing a more efficient scission process [28]. DMPA displays a higher Φ value than MTMPP, yet exhibits rather low absorbance ($249 \text{ L mol}^{-1} \text{ cm}^{-1}$), making the overall rate of radical production slower than MTMPP. In contrast, AIBN has a rather low Φ (0.4) and ϵ ($11.9 \text{ L mol}^{-1} \text{ cm}^{-1}$), resulting in the lowest radical generation rate at 365 nm.

On the basis of these considerations, MTMPP provided the fastest polymerization rate, leading to the formation of the smallest globules in short irradiation times (5 min, see Fig. S2B), and consequently large retention. Monoliths photo-initiated with DMPA required more exposure time (10 min, see Fig. S2A) to obtain monolithic network with satisfactory retention properties. SEM image of this monolith (Fig. S2A) had larger globule sizes than those commented for MTMPP (see Fig. 2SB). As we mentioned above, this result can be justified by differences in the polymerization kinetics. Although the same percentage in weight was used for all photo-initiators, the number of mmol (per 100 g) for AIBN was the highest one (6.1 versus 3.9 and 3.6 mmols for DMPA and MTMPP respectively), which can compensate partially its lowest radical generation. It allowed to obtain comparable exposure times (10 min) to those found for acetophenone-type initiators.

Also, the retention mechanism in the optimized monoliths was considered. For this purpose, the effect of ACN percentage in the mobile phase on $\log k$ for alkylbenzenes was evaluated. It was found that with an increase of ACN content produced a decrease in the retention of analytes (data not shown). This trend was consistent with RP behavior in LC. In addition, the $\log k$ values of analytes were plotted against their corresponding 1-

octanol-water coefficients. Thus, a quite straight line ($r > 0.996$) for alkylbenzenes was found for data obtained at 32% ACN mobile phase, thus indicating that the interactions of the solutes with the monolithic beds were mainly hydrophobic.

In spite of optimal irradiation exposure found for each photo-initiator, a comparison of separation performance of resulting UV-initiated monoliths was accomplished. As derived from Fig. 1 and Table 2, the photo-polymerized columns initiated with acetophenone-type initiators gave better separation performance than AIBN. Thus, the resulting efficiencies were comparable or even higher than those described in literature for these monolithic beds prepared in different housing supports. For instance, the plate heights found were better than those obtained in our previous studies using AIBN thermal-polymerized monoliths prepared in a 0.8 mm i.d. polytetrafluoroethylene (PTFE) (70-80 μm) [29] or ETFE tubing (52-100 μm) [5]. Also, our efficiencies were below 100-125 μm obtained with thermally lauryl methacrylate-based monoliths in PEEK support using comparable column dimensions (10 cm \times 1.0 mm i.d.) [30]. However, the plate heights obtained were slightly greater than that obtained (*ca.* 20 μm) for thermally BMA-based columns prepared in 0.8 mm i.d. titanium tubing (conducted at 15 $\mu\text{L min}^{-1}$ under 110°C) [31].

The quality of separation of BMA-based columns UV-polymerized using the three initiating systems considered (in their optimum conditions) was also tested using phenylurea herbicides (Fig. S3), a mixture of standard proteins (Fig. 3) and a tryptic digest of β -casein (Fig. 4). The column initiated with MTMPP gave the highest efficiency and resolution values (see Fig. S3).

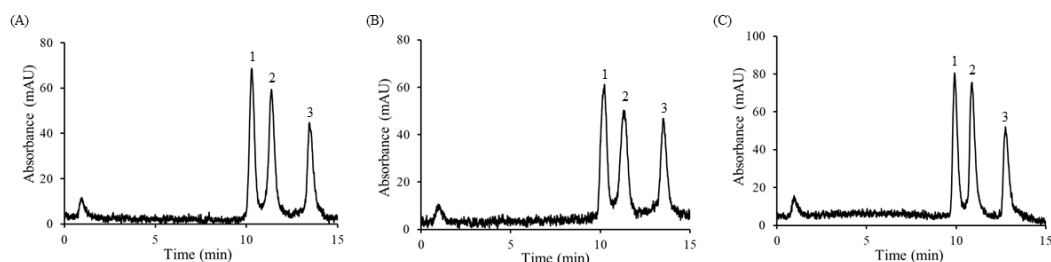


Fig. 3. Separation of proteins on BMA-based monoliths photo-polymerized with the three photo-initiators studied (at their optimal exposure conditions): (A) AIBN (365 nm - 10 min of irradiation); (B) DMPA (365 nm - 10 min); and, (C) MTMPP (365 nm - 5 min). Working LC conditions: mobile phase, A = 0.1% aqueous TFA, B = 0.1% TFA in ACN; gradient from 12 to 45% B in A in 10 min; flow rate, 0.2 mL min⁻¹; UV at 214 nm. Peak identification: (1) ribonuclease A, (2) cytochrome C and (3) myoglobin.

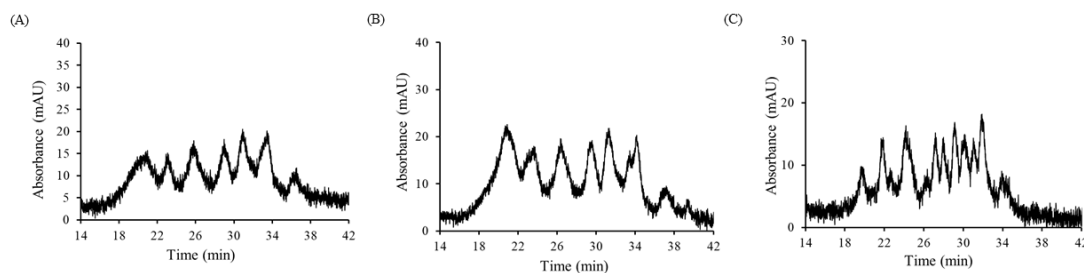


Fig. 4. Separation of a tryptic digest of β -casein using the BMA-based monoliths prepared with several photo-initiators (at the optimal exposure conditions): (A) AIBN (365 nm - 10 min of irradiation); (B) DMPA (365 nm - 10 min); and, (C) MTMPP (365 nm - 5 min). Working LC conditions: mobile phase, A = 0.1% aqueous TFA, B = 0.1% TFA in ACN; gradient from 5 to 40% B in A in 40 min; flow rate, 0.12 mL min⁻¹; injection volume, 2 μ L; UV at 214 nm.

Fig. 3 depicts the separations of the test mixture of three proteins using the same monolithic stationary phases. The performance of each monolith was evaluated in terms of peak widths measured at half peak height. MTMPP afforded the best values (17.4-19.7 s), followed by AIBN and DMPA photo-initiators (18.5-19.5 and 23.4-24.8 s, respectively). The lower permeability value of DMPA-initiated monoliths might be the reason for the lesser performance of this monolith compared with beds photo-initiated with MTMPP or AIBN.

Fig. 4 shows that the monolith synthesized with MTMPP led to much finer separation than those initiated with DMPA or AIBN. The higher efficiency of the MTMPP-initiated monolith could be ascribed to an optimal concurrence of permeability and microglobule structure.

The reproducibility of the synthesis process of the BMA-based monoliths with the three photo-initiators at their optimal irradiation time was evaluated. Thus, the run-to-run repeatability was examined using series of seven injections of the alkyl benzene test mixture, while the batch-to-batch reproducibility was evaluated by preparing three monoliths (from different polymerization mixtures). As shown in Table 3, satisfactory run-to-run repeatability in *k*- and *N*-values was found for each initiator. Batch-to-batch reproducibility obtained was also acceptable, giving the monoliths photo-polymerized with AIBN the largest RSD values.

Table 3. Repeatability and reproducibility of several chromatographic properties (expressed as RSD%) of BMA-based monolithic columns prepared with the three photo-initiators tested^a.

	AIBN		DMPA				MTMPP					
	Run-to-run (n=7)		Batch-to- batch (n=7)		Run-to-run (n=7)		Batch-to- batch (n=7)		Run-to-run (n=7)		Batch-to- batch (n=7)	
	<i>k</i>	<i>N</i>	<i>k</i>	<i>N</i>	<i>k</i>	<i>k</i>	<i>k</i>	<i>N</i>	<i>k</i>	<i>N</i>	<i>k</i>	<i>N</i>
Uracil	-	2.3	-	10.0	-	2.2	-	5.8	-	1.8	-	10.6
Toluene	1.7	1.0	2.7	8.2	1.2	1.8	7.1	8.9	0.9	1.0	5.0	7.1
Ethylbenzene	1.9	3.4	2.7	12.1	1.6	1.2	7.4	9.9	0.7	1.8	5.6	10.1
Propylbenzene	2.2	6.8	4.7	15.6	1.5	3.6	8.7	1.2	1.0	3.2	5.3	10.9
Butylbenzene	2.0	6.7	3.9	11.4	2.6	4.1	8.8	11.2	0.7	10.9	5.1	7.8
Pentylbenzene	1.8	6.0	3.7	6.8	3.1	5.0	8.9	11.0	0.7	3.4	5.4	6.8
Hexylbenzene	2.7	8.6	2.0	14.5	3.7	5.8	9.0	12.0	0.6	4.5	5.5	7.6

^a Working LC conditions as in Fig.1.

4. Conclusions

In this study, an ETFE tubing has been used as housing support to perform the photo-polymerization of BMA-based monoliths for microbore HPLC, using different free-radical initiators. The influence of each photo-initiator type (AIBN, DMPA and MTMPP) and the irradiation time was considered. The morphology of the resulting monolithic columns was investigated by SEM, and the chromatographic characteristics were evaluated by means of retention factors, efficiencies and resolution of a mixture of alkyl benzenes. As a consequence of this study, we have established that the type of initiator and exposure time can produce changes in the final globule size, and hence, variations in the chromatographic properties of monoliths. Thus, the efficiency of the polymerization process for each initiator is strongly dependent on relevant factors such as the quantum yield of dissociation and the wavelength-dependent extinction coefficient. Also, in this process, the selection of UV lamp is an important issue to allow a proper match between this source and the absorption spectra maximum wavelength of each initiator.

Under the optimal irradiation time found for each photo-initiator, similar efficiencies for the alkyl benzene mixture tested were achieved for DMPA and MTMPP; whereas the worst results were provided by AIBN. The monolithic beds were also effectively applied to the separation of phenylurea herbicides, proteins, and a trypsin digest of β -casein. In these applications, the best separation performance was obtained using MTMPP as photo-initiator, which also needed the shortest irradiation time and provided the most permeable column. Besides, it allows to increase the working flow rates and decrease the time for the separation of the solutes. The run-to-run and batch-to-batch reproducibility of monolithic beds showed slightly better RSD values for beds photo-initiated with DMPA and MTMPP than those obtained with AIBN. As far as we

know, this work is the first contribution that demonstrates the convenient use of ETFE tubing to prepare monolithic columns by photo-polymerization, being the approach described here able to be extended to the construction of stepped gradients on polymeric monolithic columns and their application in both chromatography and sample treatment field.

Acknowledgements

This research study has been sponsored by projects PROMETEO/2016/145 (Conselleria d'Educació, Investigació, Cultura i Esport, Generalitat Valenciana, Spain) and RTI2018-095536-B-I00 (Ministry of Science, Innovation and Universities, Spain).

References

- [1] M.R. Gama, F.R.P. Rocha, C.B.G. Bottoli, Monoliths: Synthetic routes, functionalization and innovative analytical applications, *TrAC Trend. Anal. Chem.* 115 (2019) 39-51.
- [2] D. Xu, Q. Wang, E. Sánchez-López, Z. Jiang, M.L. Marina, Preparation of an O-[2-(methacryloyloxy)-ethylcarbamoyl]-10,11-dihydroquinidine-silica hybrid monolithic column for the enantioseparation of amino acids by nano-liquid chromatography, *J. Chromatogr. A* 1593 (2019) 63-72.
- [3] M. Zhang, L. Gong, G. Liu, J. Kang, Preparation of a monolithic column with a mixed-mode stationary phase of reversed-phase/hydrophilic interaction for capillary liquid chromatography, *J. Sep. Sci.* 42 (2019) 662-669.
- [4] I. Ten-Doménech, H. Martínez-Pérez-Cejuela, M.J. Lerma-García, E.F. Simó-Alfonso, J.M. Herrero-Martínez, Molecularly imprinted polymers for selective solid-phase extraction of phospholipids from human milk samples, *Microchim. Acta* 184 (2017) 3389-3397.
- [5] M. Catalá-Icardo, S. Torres-Cartas, S. Meseguer-Lloret, E.F. Simó-Alfonso, J.M. Herrero-Martínez, Photografted fluoropolymers as novel chromatographic supports for polymeric monolithic stationary phases, *Talanta* 187 (2018) 216-222.

- [6] B. Fresco-Cala, E.J. Carrasco-Correa, S. Cárdenas, J.M. Herrero-Martínez, Carbon nanostructures incorporated on methacrylate monoliths for separation of small molecules by nano-liquid chromatography. *Microchemical Journal* 139 (2018) 222-229.
- [7] A. Sorribes-Soriano, F.A. Esteve-Turrillas, S. Armenta, P. Amorós, J.M. Herrero-Martínez, Amphetamine-type stimulants analysis in oral fluid based on molecularly imprinting extraction, *Anal. Chim. Acta* 1052 (2019) 73-83.
- [8] F. Svec, Porous polymer monoliths: Amazingly wide variety of techniques enabling their preparation, *J. Chromatogr. A* 1217 (2010) 902-924.
- [9] E.G. Vlakh, T.B. Tennikova, Preparation of methacrylate monoliths, *J. Sep. Sci.* 30 (2007) 2801-2813.
- [10] F. Svec, Y. Lv, Advances and Recent Trends in the Field of Monolithic Columns for Chromatography, *Anal. Chem.* 87 (2015) 250–273.
- [11] E. Frick, H.A. Ernst, D. Voll, T.J.A. Wolf, A. Unterreiner, C. Barner-Kowollik, Studying the polymerization initiation efficiency of acetophenone-type initiators via PLP-ESI-MS and femtosecond spectroscopy, *Polym. Chem.* 5 (2014) 5053-5068.
- [12] D. Nowak, J. Ortyl, I. Kamińska-Borek, K. Kukuła, M. Topa, R. Popielarz, Photopolymerization of hybrid monomers Part I: Comparison of the performance of selected photoinitiators in cationic and free-radical polymerization of hybrid monomers, *Polym. Test.* 64 (2017) 313–320.
- [13] V. Bernabé-Zafón, M. Beneito-Cambra, E.F. Simó-Alfonso, J.M. Herrero-Martínez, Comparison on photo-initiators for the preparation of methacrylate monolithic columns for capillary electrochromatography, *J. Chromatogr. A* 1217 (2010) 3231-3237.
- [14] M. Araya-Farias, M. Taverna, M. Woytasik, F. Bayle, M. Guerrouache, I. Ayed, H.H. Cao, B. Carbonnier, N.T. Tran, A new strategy for simultaneous synthesis and efficient anchorage of polymer monoliths in native PDMS microchips, *Polymer* 66 (2015) 249-258.
- [15] Green WA. *Industrial photoinitiators: a technical guide*. Boca Raton: CRC Press; 2010.
- [16] A. Eibel, D.E. Fast, G. Gescheidt, Choosing the ideal photoinitiator for free radical photopolymerizations: predictions based on simulations using established data, *Polym. Chem.* 9 (2018) 5107-5115.
- [17] Z. Liu, G. Zhang, W. Lu, Y. Huang, J. Zhang, UV light-initiated RAFT polymerization induced self-assembly, T. Chen. *Polym. Chem.* 6 (2015) 6129-6132.

- [18] A. Escrig-Doménech, I. Ten-Doménech, E.F. Simó-Alfonso, J.M. Herrero-Martínez, Preparation and characterization of octadecyl acrylate monoliths for capillary electrochromatography by photochemical, thermal, and chemical initiation, *J. Sep. Sci.* 36 (2013) 2283–2290.
- [19] A. Kobayashi, T. Nakaza, T. Hirano, S. Kitagawa, H. Ohtani, Variation in the chromatographic, material, and chemical characteristics of methacrylate-based polymer monoliths during photoinitiated low-temperature polymerization, *J. Sep. Sci.* 39 (2016) 2459–2465.
- [20] R.J. Vonk, S. Wouters, A. Barcaru, G. Vivó-Truyols, S. Eeltink, L.J. de Koning, P.J. Schoenmakers, Post-polymerization photografting on methacrylate-based monoliths for separation of intact proteins and protein digests with comprehensive two-dimensional liquid chromatography hyphenated with high-resolution mass spectrometry, *Anal. Bioanal. Chem.* 407 (2015) 3817-3829.
- [21] H. Wang, H. Zhang, Y. Lv, F. Svec, T. Tan, Polymer monoliths with chelating functionalities for solid phase extraction of metal ions from water, *J. Chromatogr. A* 1343 (2014) 128–134.
- [22] P. Rattanakit, S. Liawruangrath, Performance evaluation of monolith based immobilized acetylcholinesterase flow-through reactor for copper(II) determination with spectrophotometric detection, *Journal of Chemistry* 2014 (2014) 1-7.
- [23] K. Flook, Y. Agroskin, C. Pohl, Reversed-phase monoliths prepared by UV polymerization of divinylbenzene, *J. Sep. Sci.* 34 (2011) 2047–2053.
- [24] E.G. Leggesse, W.R. Tong, S. Nachimuthu, T.Y. Chen, J.C. Jiang, Theoretical study on photochemistry of Irgacure 907, *J. Photochem. Photobiol. A: Chem.* 347 (2017) 78–85.
- [25] J. Krenkova, F. Foret, Nanoparticle-modified monolithic pipette tips for phosphopeptide enrichment, *Anal. Bioanal. Chem.* 405 (2013) 2175–2183.
- [26] Open chemistry database at the National Institutes of Health. <https://pubchem.ncbi.nlm.nih.gov/compound/2_2_-Azobis_2-methylpropionitrile> (accessed 26 June 2019).
- [27] E. Yousif, R. Haddad, Photodegradation and photostabilization of polymers, especially polystyrene: review, *Springerplus.* 2 (2013) 398.
- [28] W.A. Green. *Industrial photoinitiators: a technical guide.* Boca Raton: CRC Press; 2010.

- [29] M. Catalá-Icardo, S. Torres-Cartas, S. Meseguer-Lloret, C. Gómez-Benito, E. Carrasco-Correa, E.F. Simó-Alfonso, G. Ramis-Ramos, J.M. Herrero-Martínez, Preparation of organic monolithic columns in polytetrafluoroethylene tubes for reversed-phase liquid chromatography, *Anal. Chim. Acta* 960 (2017) 160-167.
- [30] S. Shu, H. Kobayashi, N. Kojima, A. Sabarudin, T. Umemura, Preparation and characterization of lauryl methacrylate-based monolithic microbore column for reversed-phase liquid chromatography, *J. Chromatogr. A* 1218 (2011) 5228– 5234.
- [31] E.P. Nesterenko, P.N. Nesterenko, D. Connolly, F. Lacroix, B. Paull, Micro-bore titanium housed polymer monoliths for reversed-phase liquid chromatography of small molecules, *J. Chromatogr. A* 1217 (2010) 2138-2146.